Icarus 215 (2011) 197–203

Contents lists available at ScienceDirect

Icarus

journal homepage: www.elsevier.com/locate/icarus

Vertical profile of H_2SO_4 vapor at 70–110 km on Venus and some related problems

Vladimir A. Krasnopolsky *

Department of Physics, Catholic University of America, Washington, DC 2006, United States

ARTICLE INFO

Article history:
Received 27 February 2011
Revised 24 June 2011
Accepted 24 June 2011
Available online 3 July 2011

Keywords:
Venus
Venus, Atmosphere
Photochemistry
Abundances, Atmospheres
Atmospheres, Composition

ABSTRACT

The vertical profile of H_2SO_4 vapor is calculated using current atmospheric and thermodynamic data. The atmospheric data include the H_2O profiles observed at 70–112 km by the SOIR solar occultations, the SPICAV-UV profiles of the haze extinction at 220 nm, the VeRa temperature profiles, and a typical profile of eddy diffusion. The thermodynamic data are the saturated vapor pressures of H_2O and H_2SO_4 and chemical potentials of these species in sulfuric acid solutions. The calculated concentration of sulfuric acid in the cloud droplets varies from 85% at 70 km to a minimum of 70% at 90 km and then gradually increasing to 90–100% at 110 km. The H_2SO_4 vapor mixing ratio is $\sim 10^{-12}$ at 70 and 110 km with a deep minimum of 3×10^{-18} at 88 km. The H_2O–H_2SO_4 system matches the local thermodynamic equilibrium conditions up to 87 km. The column photolysis rate of H_2SO_4 is 1.6×10^5 cm^{-2} s^{-1} at 70 km and 23 cm^{-2} s^{-1} at 90 km. The calculated abundance of H_2SO_4 vapor at 90–110 km and its photolysis rate are smaller than those presented in the recent model by Zhang et al. (Zhang, X., Liang, M.C., Montmessin, F., Bertaux, J.L., Parkinson, C., Yung, Y.L. [2010]. Nat. Geosci. 3, 834–837) by factors of 10^6 and 10^9, respectively. Assumptions of 100% sulfuric acid, local thermodynamic equilibrium, too warm atmosphere, supersaturation of H_2SO_4 (impossible for a source of SO_X), and cross sections for $H_2SO_4 \cdot H_2O$ (impossible above the pure H_2SO_4) are the main reasons of this huge difference. Significant differences and contradictions between the SPICAV-UV, SOIR, and ground-based submillimeter observations of SO_X at 70–110 km are briefly discussed and some weaknesses are outlined. The possible source of high altitude SO_X on Venus remains unclear and probably does not exist.

1. Introduction

Ground-based submillimeter observations of the SO_2 and SO lines (Sandor et al., 2010) in 2004–2008 revealed significant abundances of these species on Venus at 84–100 km. SO_2 varied in 21 observations at different local times at the Venus disk center from 0 to 76 ppb with a mean value of 23 ppb, and the abundances of SO were from 0 to 31 ppb with a mean of 7.5 ppb. According to the observations, both SO_2 and SO are much more abundant at 84–100 km than at 70–84 km. This behavior requires a high-altitude source of SO_X on Venus.

Vertical profiles of SO_2 in the mesosphere of Venus were measured by solar occultations from the Venus Express orbiter. Observations of the SO_2 lines near 3.98 μm using the SOIR spectrograph (Belyaev et al., 2008, 2010) show a decrease in the SO_2 mixing ratio from 65 to 80 km by one or two orders of magnitude with typical values of 10–30 ppb at 80 km. The lines become very weak and unobservable above 80 km. Observations of the SO_2 bands near 210 nm using SPICAV-UV gave vertical profiles of SO_2 from 90 to 110 km with typical values of 100–1000 ppb throughout this altitude range (Belyaev et al., 2010). The SPICAV-UV observations of SO_2 are impossible above 110 km because of the very low number densities of SO_2. These observations are also impossible below 90 km because "the aerosol extinction is too strong below 90 km in the UV to register any solar signal" (Belyaev et al., 2010). Here we do not discuss a history of the nadir observations of SO_2 on Venus and its long-term variations (Esposito et al., 1988). The latest nadir observations using SPICAV-UV (Marcq et al., 2011) show highly variable SO_2 column abundances with typical SO_2 mixing ratios of 100–1000 ppb. Ground-based high-resolution spectroscopy at 4.04 μm gave a mean mixing ratio of 350 ± 50 ppb at 72 km (Krasnopolsky, 2010a). These data agree with the SOIR occultations (Belyaev et al., 2008, 2010).

Though there are significant differences and even contradictions between the observations of vertical profiles of SO_2, both ground-based submillimeter and Venus Express observations indicate a high-altitude source of SO_X. A photochemical model with photolysis of H_2SO_4 vapor as such a source was recently developed by Zhang et al. (2010). To fit the observations of SO_2 and SO, the model requires very large abundances of H_2SO_4 vapor that reach 1–10 ppm near 100 km.

However, there are sufficient data on the composition and properties of the Venus atmosphere to calculate a vertical profile of

* Address: 6100 Westchester Park Drive #911, College Park, MD 20740, USA.
E-mail address: vlad.krasn@verizon.net

0019-1035/$ - see front matter © 2011 Elsevier Inc. All rights reserved.
doi:10.1016/j.icarus.2011.06.036

H_2SO_4 vapor with a reasonable accuracy. That will be a subject of this paper, and then we will discuss the results and compare with some data from Zhang et al. (2010).

2. Vertical profile of H_2SO_4 vapor

2.1. Thermodynamic data

For phase equilibrium between liquid or solid sulfuric acid and H_2O and H_2SO_4 vapors, their partial pressures are equal to

$$\ln p_i = \ln p_{si} + \frac{\mu_i - \mu_i^o}{RT}, \qquad (*)$$

(see, e.g., Krasnopolsky and Pollack, 1994). Here subscript $i = 0$ and 1 refers to H_2O and H_2SO_4, respectively, subscript s means saturated vapor, R is the gas constant, T is temperature, and $\mu_i - \mu_i^0$ is the difference of chemical potentials of a species in solution and a pure species. Chemical potentials of H_2O and H_2SO_4 in sulfuric acid as functions of its concentration are given in Giauque et al. (1960) and Zeleznik (1991). They are shown in Fig. 1.

Murphy and Koop (2005) describe the saturated vapor pressure of H_2O over ice by the following relationship:

$$\ln p_{S0}\ (\text{bar}) = -1.96250 - 5723.265/T + 3.53068 \ln T - 0.00728332T.$$

This function for the temperature range of 150–300 K is shown in Fig. 1.

The saturated pressure of H_2SO_4 vapor was measured by Stull (1947) at 420–580 K, Ayers et al. (1980) at 338–445 K, and Richardson et al. (1986) at 263–303 K. The H_2SO_4 vapor densities at 338 and 263 K are smaller than that at 420 K by factors of 300 and 10^6, respectively, and the lowering of the temperature range required much more sensitive laboratory methods. There are some differences between the data from those papers. We will use the results of Richardson et al. (1986) because their sensitivity was much better than those in the previous works and their temperature range is closer to that in the Venus mesosphere. Richardson et al. (1986) measured H_2SO_4 vapor pressure above sulfuric acid with weight concentration of 98.479%, which was equal to

$$\ln p_{S1}\ (\text{bar}) = 14.07 - 9360/T.$$

Our correction to the pure H_2SO_4 acid using the chemical potentials from Giauque et al. (1960) gives

$$\ln p_{S1}\ (\text{bar}) = 14.07 - 9317/T.$$

This function is shown in Fig. 1 in the temperature range of 150–300 K. The vapor pressure of H_2SO_4 is smaller than that of H_2O by a factor of $\sim 10^8$ at 200 K.

2.2. Some data on the atmosphere of Venus

The vertical profiles of H_2O, HDO, and CO_2 in the altitude range of 70–112 km were measured by solar occultations from Venus Express using the SOIR spectrograph (Fedorova et al., 2008). The analyzed profiles were observed at 22 locations at latitudes 63–88°N. A mean of those H_2O profiles is shown in Fig. 2. There are no published H_2O profiles at the middle and low latitudes. However, the observed H_2O profiles do not show any latitude trend within 63–88°N (see Fig. 12 in Fedorova et al. (2008)) and may be rather typical of the Venus atmosphere.

For the conditions of the H_2O observations we choose a mean of four temperature profiles measured by radio occultations from Venus Express (Tellmann et al., 2009) at latitudes 81–88°N. The profile is in the $T(p)$ format, and its conversion to $T(z)$ and $p(z)$ may be made by integration of the barometric formula:

$$\frac{dp}{p} = -\frac{dz}{H} = -\frac{mg_0 dz}{kT(p)\left(1+\frac{z}{R_0}\right)^2}; \quad x = \frac{z}{1+\frac{z}{R_0}} = -\frac{k}{mg_0}\int_{p_0}^{p} T(p)\frac{dp}{p};$$

$$z = \frac{x}{1 - x/R_o},$$

and $k/mg_0 = 2207.5$ cm/K for $z_0 = 70$ km ($R_0 = 6122$ km).

The obtained temperature and density profiles are shown in Fig. 2. Temperature profiles measured by radio occultations and thermal inversion of the CO_2 band at 15 μm extend typically up to 100 km. The profile is extrapolated to 110 km using some data from Bougher et al. (2010).

The H_2O mixing ratio in the SOIR observations is almost constant at ~1 ppm in the altitude range of 75–105 km (Fig. 2). Yung and DeMore (1982) adopted the same H_2O mixing ratio for 56–112 km in their photochemical models three decades ago.

Properties of haze in the mesosphere of Venus were studied from the Venera 9 and 10 (Krasnopolsky, 1980, 1983, 1986), Pioneer Venus (Lane and Opstbaum, 1983), and Venus Express (Wilquet et al., 2009; de Kok et al., 2011) orbiters. There is a reasonable mutual agreement between these publications. We choose a profile of the haze extinction coefficient at 220 nm observed by

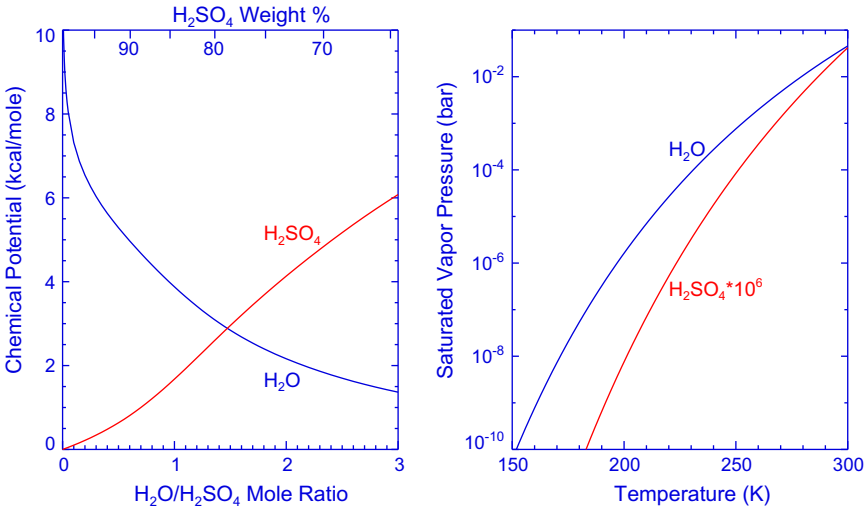

Fig. 1. Left panel: negative chemical potentials of H_2O and H_2SO_4 as functions of the H_2O/H_2SO_4 mole ratio in the sulfuric acid solution relative to the pure substances (Giauque et al., 1960). Right panel: saturated vapor pressures of H_2O and H_2SO_4 as functions of temperature.

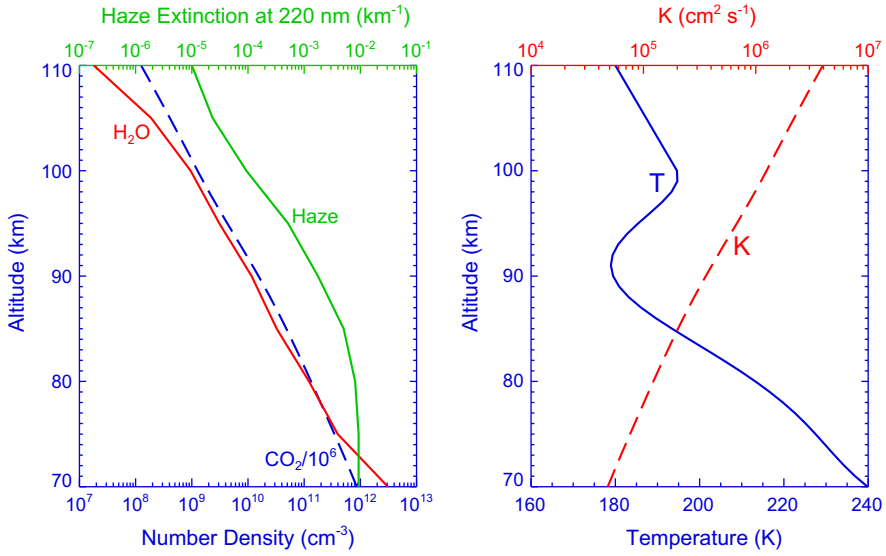

Fig. 2. Left panel: vertical profiles of H_2O and CO_2 densities and haze extinction at 220 nm. The H_2O profile is a mean of 22 profiles measured using SOIR at Venus Express at latitudes 63–88°N (Fedorova et al., 2008). The haze extinction was observed by SPICAV-UV at 70°N (Wilquet et al., 2009). Right panel: mean of four temperature profiles measured by radio occultations from Venus Express near 85°N (Tellmann et al. 2009). The mean profile extends to 100 km and is extrapolated to 110 km. The CO_2 profile in the left panel corresponds to this temperature profile. Profile of eddy diffusion coefficient K is from Krasnopolsky and Parshev (1981, 1983).

solar occultations using SPICAV-UV near 70°N from Fig. 6a in Wilquet et al. (2009). This profile is shown in Fig. 2.

We adopt a profile of eddy diffusion coefficient K (Fig. 2) from the model by Krasnopolsky and Parshev (1981, 1983). Eddy diffusion in Zhang et al. (2010) is rather similar to this profile with a typical difference within a factor of 2.

2.3. Calculated profiles of H_2SO_4 concentration and vapor density

Assuming local thermodynamic equilibrium (LTE) between the sulfuric acid aerosol and H_2O and H_2SO_4 vapors, vertical profiles of the weight concentration of sulfuric acid in the cloud droplets (hereafter concentration) and H_2SO_4 vapor may be calculated using the H_2O and T profiles shown in Fig. 2. This can be made using relationship (∗); the thermodynamic data from Fig. 1 are only required and result in the profiles of concentration and H_2SO_4 vapor shown in Fig. 3. The calculated concentration is equal to ~85% at 70–80 and 100–110 km with a minimum of 70% near 90 km.

The LTE is established via a balance of condensation and sublimation of H_2O and H_2SO_4, and the atmospheric mixing and photolyses of these species tend to break the LTE. Here we will assess all these processes.

The extinction ratio $k = \sigma/\pi r^2$ is equal to ~2 for large aerosol particles with $2\pi r/\lambda \gg 1$. Here σ is the particle extinction cross section, r is its radius, and λ is the wavelength. That is why we chose the haze extinction profile in Fig. 2 at the shortest available wavelength. A more accurate approximation for the extinction ratio is

$$k = 2 - \frac{4}{y}\sin y + \frac{4}{y^2}(1 - \cos y); \quad y = \frac{4\pi r(m_r - 1)}{\lambda}$$

(van de Hulst, 1957; see also Krasnopolsky, 1986, p. 104). Here m_r is the real refractive index of the particle substance that is equal to

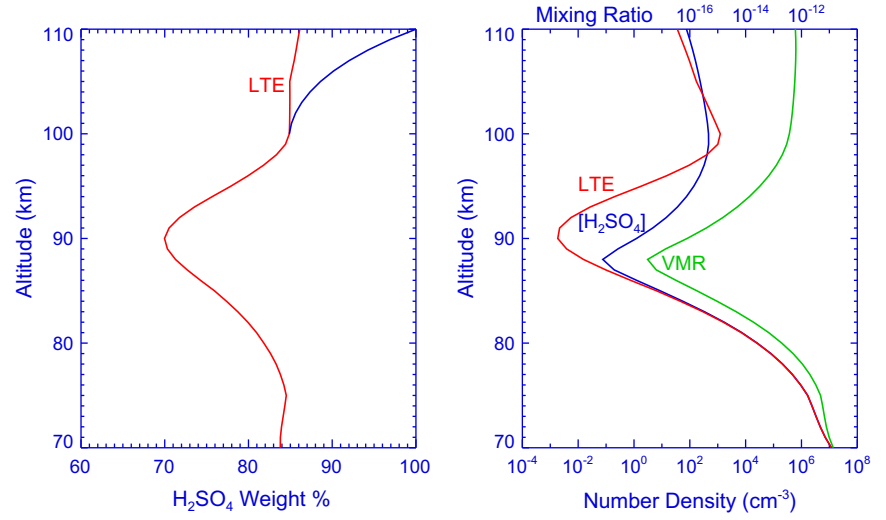

Fig. 3. Left panel: profiles of concentration of the sulfuric acid aerosol in the haze on Venus for LTE and true conditions. Right panel: profiles of the number density and volume mixing ratio of H_2SO_4 vapor on Venus. H_2SO_4 number densities for LTE are shown as well.

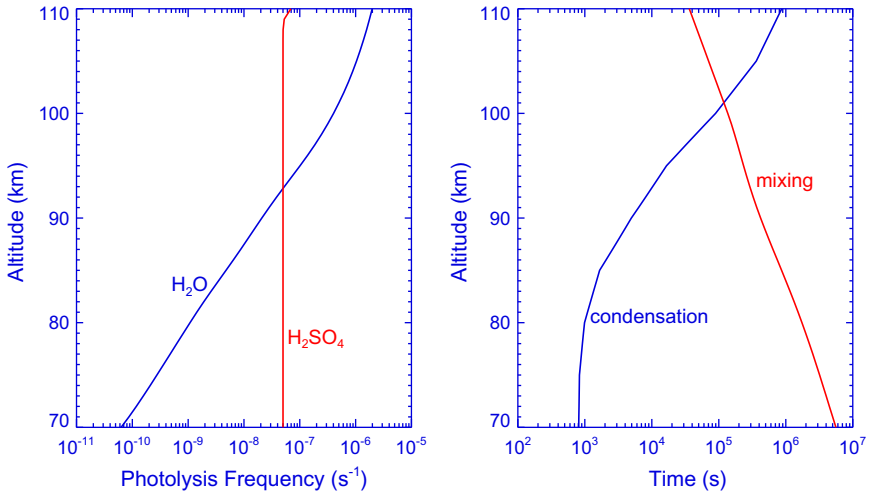

Fig. 4. Photolysis frequencies for H_2O and H_2SO_4 vapors (left panel) and comparison of times of condensation and mixing for H_2O (right panel).

1.55 for sulfuric acid in Venus' mesosphere (Wilquet et al., 2009). This expression gives $k \approx 2$ as a reasonable approximation for the observed haze particle size in the range of $r = 0.1$–1 μm. Then the specific area of the haze $S = 4\pi r^2 n_a$ is just the haze extinction coefficient (Fig. 2) converted to cm^{-1} and scaled by a factor of 2; n_a is the particle number density. Using the observed haze extinction profile (Fig. 2), we avoid microphysical modeling of the processes of the haze formation, removal, and transport.

The condensation flux $\beta_i n_{ei} V_i/4$ is equal to flux of sublimation for thermodynamic equilibrium. Here n_{ei} is the vapor density of H_2O or H_2SO_4 under thermodynamic equilibrium, $V_i = (8kT/\pi m_i)^{1/2}$ is the mean thermal velocity, and β_i is the uptake coefficient which is ~0.5 (Sander et al., 2006). This flux times the haze specific area gives a local production of H_2O or H_2SO_4 in the atmosphere; this relationship with n_i instead of n_{ei} gives a local condensation rate.

Photolysis of H_2O is calculated using the known solar UV spectrum at 110–220 nm (Woods et al., 1996) and CO_2 and H_2O absorption cross sections (Parkinson et al., 2003; Cheng et al., 1999). The photolysis frequency of H_2SO_4 by the visible light is 5×10^{-8} s^{-1} at 1 AU, and its cross section has a strong peak of 6×10^{-17} cm^2 (Lane and Kjaergaard, 2008) at Lyman-alpha (122 nm). The photolysis frequencies I_i are calculated for the global-mean conditions, that is, for solar zenith angle of 60° and reduced by a factor of 2 to account for the night side. They are shown in Fig. 4. The solar Lyman-alpha is mostly absorbed above 110 km and weakly affects the atmosphere in our altitude range.

The assumption of LTE is valid if the time of condensation $\tau_{c0} = (\beta_0 V_0 S/4)^{-1}$ is shorter than the mixing time $\tau_m = H^2/K$; the photolysis lifetime is much longer than these times and its effect is low. Comparison of the two times is shown in Fig. 4 (right panel), and they become equal at 100 km. To calculate true vertical profiles of H_2O and H_2SO_4 vapors, we need to solve the steady-state one-dimensional continuity equations for H_2O and H_2SO_4 vapors. The equations include sources from sublimation of the species, sinks in the condensation and photolysis processes, and vertical transport by eddy diffusion. The equations are solved using a method described in Krasnopolsky and Cruikshank (1999) in the altitude range of 70–110 km with a step of 1 km. H_2O and H_2SO_4 densities at the lower boundary are those for LTE; velocities at the upper boundary are equal to $I_0 H \approx 2$ cm s^{-1} for H_2O and zero for H_2SO_4.

The concentration of sulfuric acid aerosol droplets as a function of altitude is a variable in our problem to fit the measured profile of H_2O in Fig. 2. The solution confirms the expectation that deviations of the concentration from LTE are very small below 100 km and significant above this altitude. The H_2O scale height at 105–110 km is smaller than that below 100 km by a factor of 2. This feature may be simulated by increase of either the concentration of the sulfuric acid droplets to ~100% or the diffusion velocity of H_2O at the upper boundary. We choose the former (Fig. 3) to agree better with Zhang et al. (2010). Our basic conclusions are not sensitive to this choice.

Calculated profiles of the H_2SO_4 number density are shown in Fig. 3 (right panel) for the LTE and true conditions. The profiles of H_2O are very similar to that in Fig. 2 and not shown. It is interesting to note that for the concentration of 100% at 110 km the LTE densities of H_2O and H_2SO_4 would be smaller by a factor of 5×10^9 and larger by a factor of 23, respectively, than those observed and calculated. That is, H_2O is supersaturated relative to the sulfuric acid haze by a factor of 5×10^9, although it is far below the saturation level for pure water. This means that the assumption of LTE is inapplicable to the H_2O–H_2SO_4 mixture at 110 km. Actually the concentration of sulfuric acid is rather uncertain at 105–110 km in our model.

The aerosol specific area is low and eddy diffusion is rather strong at 110 km (Fig. 4, right). Eddy diffusion smoothes the profile of H_2SO_4 which is rather similar to that for LTE at 97–110 km. The minimum is not so deep as that for LTE and shifted down from 90 to 88 km. The H_2SO_4 vapor mixing ratio is equal to $\sim 10^{-12}$ at both boundaries of 70 and 110 km with a deep minimum of 3×10^{-18} at 88 km.

Uncertainties of the calculated profile of H_2SO_4 vapor are caused by those of the H_2SO_4 saturated vapor pressure (Richardson et al., 1986), the adopted H_2O and H_2SO_4 uptake coefficients (Sander et al., 2006), and eddy diffusion. The uncertainty of the H_2SO_4 saturated vapor pressure may reach an order of magnitude near 200 K and directly affects the H_2SO_4 profile by the same factor. The calculated H_2SO_4 profile below 88 km is similar to that for LTE and insensitive to the adopted uptake coefficient and eddy diffusion. If eddy diffusion is larger than that in Fig. 2 by a factor of 10, then the H_2SO_4 density is smaller at 98–110 km by a factor of ~5 and larger near the minimum by two orders of magnitude. The H_2SO_4 densities at 98–110 km are approximately proportional to the uptake coefficient. Overall, the H_2SO_4 densities at 95–110 km are uncertain within a factor of ~20.

The photolysis of H_2SO_4 vapor weakly affects its density. The column photolysis rate is 1.6×10^5 cm^{-2} s^{-1}, and the column rate at 90–110 km is 23 cm^{-2} s^{-1}. These may be compared with the

column photolysis rate of CO_2 that is equal to 3.4×10^{12} cm^{-2} s^{-1} above 80 km (Krasnopolsky, 2010b). Therefore, the photochemical effect of H_2SO_4 vapor is weak.

3. Comparison with some data from photochemical model by Zhang et al. (2010)

We discussed in the Introduction that the model by Zhang et al. (2010, hereafter Model 1) was aimed to simulate high abundances of SO_2 measured in the Venus atmosphere in the submillimeter range (Sandor et al., 2010) and by solar occultations using SPICAV-UV (Belyaev et al., 2010). Zhang et al. (2010) correctly concluded that those observations require a high-altitude source of SO_X and suggested photolysis of H_2SO_4 (and/or sulfur aerosol) as this source. This suggestion looked reasonable because of the lack of any alternative ideas for high-altitude source of SO_X. We will discuss below the quantitative differences between our simple calculations and Model 1 that appear very significant and rule out the basic idea of Model 1.

3.1. Temperature profile

According to the SPICAV-UV stellar occultations (Bertaux et al., 2007), the nighttime temperature profile has a peak near 100 km that increases from 190 K at solar zenith angle of 110° to 230 K near the antisolar point. This is a new method to measure temperature profiles on Venus and Mars using the UV absorption of CO_2, and this method covers a gap between the radio occultations and the CO_2 spectroscopy at 15 and 4.3 μm below 100 km and the Pioneer Venus mass spectrometer and atmospheric drag measurements above 135 km. Only a mean temperature might be obtained in the gap of 100–135 km by comparing the densities at its boundaries.

However, all methods except the UV stellar occultation do not support the nighttime temperatures significantly exceeding 200 K near 100 km. For example, the Venus Express radio occultations (Tellmann et al., 2009) and a recent review of temperature profiles from the IR spectroscopy at 15 μm onboard Venera 15 (Zasova et al., 2006) do not show high temperatures near 100 km. The problem may be partly due to both continuum and line absorption of CO_2 in the UV range. Properties of the CO_2 lines and their curves of growth are poorly known in this range, laboratory measurements of the CO_2 cross sections are made at pressure exceeding that near 100 km on Venus, and that may be a source of error.

Ground-based high-resolution spectroscopic observations of the O_2 nightglow at 1.27 μm by five independent teams revealed a mean rotational temperature of 187 ± 3 K (Krasnopolsky, 2010b). For a radiative lifetime of the upper state of 1.2 h, the rotational temperature should be equal to kinetic temperature of the nightglow peak at 95–100 km. A general circulation model for the upper atmosphere ($h > 80$ km) on Venus (Bougher et al., 2010) gives a temperature maximum of 205 K at 110 km at the antisolar point.

Model 1 adopts a maximal nighttime temperature observed by SPICAV-UV (Bertaux et al., 2007). Its peak of 234 K (245 K in their Fig. S2a) at 98 km is much above the mean data for the night side. Furthermore, this profile is inapplicable for the calculations of photolysis of H_2SO_4 that occurs on the day side.

3.2. Profile of H_2SO_4 and its photolysis rate

Model 1 adopts a concentration of the sulfuric acid aerosol particles of 75% at 70–90 km and 100% at 90–112 km. H_2O densities above the pure sulfuric acid haze at 90–110 km would be extremely low, smaller than those observed by SOIR (Fig. 2) by many orders of magnitude. We have checked this case using both LTE and the steady-state model.

Vaida et al. (2003) estimated photolysis frequencies of sulfuric acid monohydrate $H_2SO_4 \cdot H_2O$ by the visible light as exceeding those for H_2SO_4 by two orders of magnitude, and Model 1 adopts this estimate to calculate the H_2SO_4 photolysis rate. However, monohydrate $H_2SO_4 \cdot H_2O$ is completely lacking above the pure sulfuric acid, and this increase of the photolysis rate in Model 1 by a factor of 100 is unmotivated.

To fit the SPICAV-UV measurements of SO_2, Model 1 adopts supersaturation of H_2SO_4 at 90–112 km by a factor of 10. However, supersaturation may occur if local production of H_2SO_4 exceeds its local loss, that is, in the case of a local sink but not a source of SO_X. Again, this factor of 10 should be removed.

Model 1c results in a column photolysis rate of H_2SO_4 of 2.8×10^{10} cm^{-2} s^{-1} at 90–110 km. It is larger than that calculated in this paper by a factor of 10^9. The adoptions of the pure H_2SO_4 haze, the LTE conditions, and the temperature profile that is higher by ~50 K than the mean observational data contribute $\sim 10^6$ to this overestimation.

4. Observations of SO_2 and related problems

Thus we conclude that H_2SO_4 vapor cannot be a high-altitude source of SO_X to explain the SO_2 behavior in the SPICAV-UV and SOIR solar occultation observations. It is mentioned in Model 1 that sulfur aerosol S_X may also be a source of SO_X; however, inspection of production of S_X in the photochemical model by Mills (1998) rules out a source that may be comparable with the required value of 2.8×10^{10} cm^{-2} s^{-1} above 90 km. We do not have any alternative ideas on a significant source of SO_X above 90 km as well.

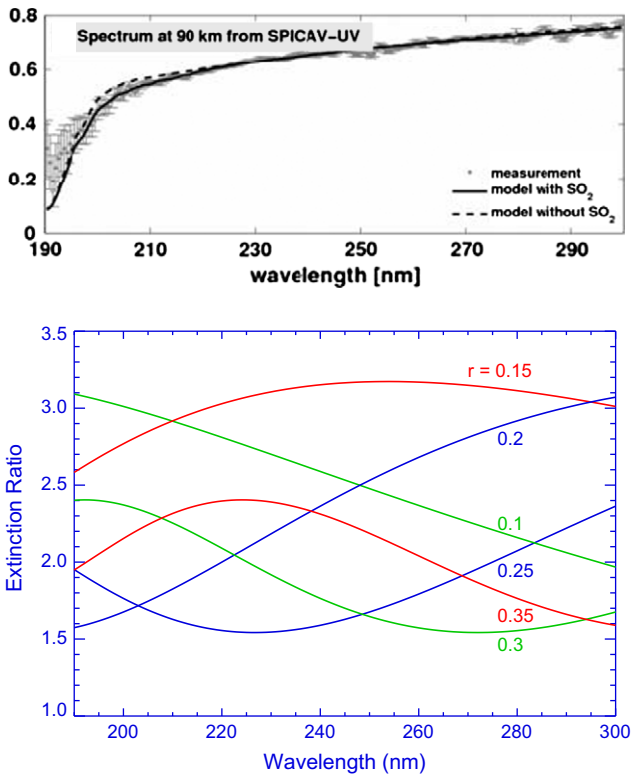

Fig. 5. SPICAV observations of SO_2 (upper panel, from Belyaev et al. (2010)). The spectrum uncertainties are gray. Lower panel: UV spectra of extinction ratio $\sigma/\pi r^2$ (σ is the extinction cross section) of sulfuric acid aerosol particles for various particle radius r in μm. The spectra are calculated for refractive index 1.55.

There are significant differences and contradictions between the SPICAV-UV solar occultation data on SO_2 and the submillimeter observations of SO_2 and SO (Sandor et al., 2010) that are discussed in that paper. Actually there is no refereed publication on the SPICAV-UV profiles of SO_2, and our consideration is based on the extended abstract by Belyaev et al. (2010). They show one of the observed SPICAV-UV spectra which is copied in Fig. 5 (upper panel). The lower panel demonstrates the calculated extinction spectra of sulfuric acid aerosol particles with refractive index 1.55 for various particle radii from 0.1 to 0.35 μm. An increase in extinction at 200–220 nm is seen for $r = 0.25$–0.35 μm, and we feel that it is possible to fit the observed spectrum by a proper choice of the particle radii with no SO_2. We do not rule out that the haze particles with $r \approx 0.1$ μm may explain the decline in the spectral transmission to the blue while adding of the particles with $r \approx 0.3$ μm may substitute the SO_2 absorption. The refractive index may also vary with wavelength, concentration, and temperature giving additional degrees of freedom for fitting. Both spectral fits with and without SO_2 are poor at 190–200 nm.

The haze extinction coefficient at 220 nm is $\alpha \approx 0.002$ km^{-1} at 90 km and its scale height is $H_e = 3.4$ km (Fig. 2). Then the slant extinction optical depth on the limb is $\tau = \alpha\,(2\pi R H_e)^{1/2} = 0.7$ for $R = 6142$ km at $h = 90$ km. The authors' statement that "the aerosol extinction is too strong below 90 km in the UV to register any solar signal" is therefore not justified, and it is not clear why the SO_2 mixing ratio could not been retrieved below 90 km.

The SO_2 mixing ratios are much smaller in the submillimeter observations with a mean value of 23 ppb above 84 km (Sandor et al., 2010), and the required source of SO_X is smaller than that in Model 1c by a factor of ~50. However, the calculated profile of H_2SO_4 vapor cannot support even this reduced source. We see two problems in the submillimeter observations of SO_2. First of all, their mean value of 23 ppb above 84 km is similar to 10–30 ppb from the SOIR observations near 80 km (Belyaev et al., 2010). However, the SOIR mixing ratios are increasing to 70 km by an order of magnitude, while the submillimeter observations require a steep decrease in SO_2 below 84 km. The standard photochemistry supports the former and disagrees with the latter.

Another problem is a high short-term variability of the submillimeter abundances of SO_X in the global scale. For example, the SO_2 abundances in two consecutive days 20 and 21 January 2007 increased by a factor of 2.7 while the SO abundance decreased by the same factor so that their sum is almost the same. This could be understandable in term of dynamics for local variability. However, the instrument field of view covered the full disk of Venus. The similar problem is for the submillimeter observations of H_2O on Venus (Sandor and Clancy, 2005) where the global H_2O varied by more than an order of magnitude within intervals of a few months.

There are some observational data that have remained unexplained for decades. For example, the high afternoon water from the Pioneer Venus infrared radiometer observations was recently confirmed in a thorough analysis by Koukouli et al. (2005) but disagrees with all later observations of water near the cloud tops.

5. Conclusions

Current atmospheric and thermodynamic data are applied to calculate the vertical profile of H_2SO_4 vapor. The atmospheric data are the profiles of H_2O observed at 70–112 km by the SOIR solar occultations, the SPICAV-UV profiles of the haze extinction at 220 nm, the VeRa temperature profiles, and a typical profile of eddy diffusion. The thermodynamic data are the saturated vapor pressures of H_2O and H_2SO_4 and chemical potentials of these species in sulfuric acid solutions. Using the haze extinction profile, we avoid microphysical modeling of the haze formation, loss, and transport.

The calculated concentration of sulfuric acid in the cloud droplets varies from 85% at 70 km to a minimum of 70% at 90 km and then gradually increasing to 90–100% at 110 km. The calculated H_2SO_4 vapor mixing ratio is $\sim 10^{-12}$ at 70 and 110 km with a deep minimum of 3×10^{-18} at 88 km. The H_2O–H_2SO_4 system matches the local thermodynamic equilibrium conditions up to 87 km. The column photolysis rate of H_2SO_4 is 1.6×10^5 cm^{-2} s^{-1} at 70 km and 23 cm^{-2} s^{-1} at 90 km.

The calculated abundance of H_2SO_4 vapor at 90–110 km and its photolysis rate are smaller than those in the recent model by Zhang et al. (2010) by factors of 10^6 and 10^9, respectively. This huge difference appears because of the assumptions of 100% sulfuric acid, local thermodynamic equilibrium, too warm atmosphere, supersaturation of H_2SO_4 (impossible for a source of SO_X), and cross sections for $H_2SO_4 \cdot H_2O$ (impossible above the pure H_2SO_4).

There are significant differences and contradictions between the SPICAV-UV, SOIR, and ground-based submillimeter observations of SO_X at 70–110 km. They are briefly discussed and some weaknesses are outlined. There are no good ideas for a high-altitude source of SO_X on Venus.

References

Ayers, G.P., Gillett, R.W., Gras, J.L., 1980. On the vapor pressure of sulfuric acid. Geophys. Res. Lett. 7, 433–436.

Belyaev, D., Korablev, O., Fedorova, A., Bertaux, J.-L., Vandaele, A.-C., Montmessin, F., et al., 2008. First observations of SO_2 above Venus clouds by means of solar occultation in the infrared. J. Geophys. Res. 113, E00B25. doi:10.1029/2008JE003143.

Belyaev, D., Marcq, E., Montmessin, F., Bertaux, J.L., Mahieux, A., Korablev, O., et al., 2010. SO_2 observations above Venus' clouds by SPICAV/SOIR from the VEX orbiter. 2010 VEXAG International Workshop, Madison, USA (CD-ROM).

Bertaux, J.L. et al., 2007. A warm layer in Venus' cryosphere and high-altitude measurements of HF, HCl, H_2O and HDO. Nature 450, 646–649.

Bougher, S.W., Brecht, A., Parkinson, C., Rafkin, S., Gerard, J.C., 2010. Dynamics, O_2 nightglow, and ion-neutral chemistry of the Venus upper atmosphere: Interpretation of Venus Express datasets using the VTGCM. 2010 VEXAG International Workshop, Madison, USA (CD-ROM).

Cheng, B.M., Chew, E.P., Liu, C.P., Bahou, M., Lee, Y.P., Yung, Y.L., et al., 1999. Photo-induced fractionation of water isotopomers in the martian atmosphere. Geophys. Res. Lett. 26, 3657–3660.

De Kok, R., Irwin, P.G.J., Tsang, C.C., Piccioni, G., Drossart, P., 2011. Scattering particles in nightside limb observations of Venus' upper atmosphere by Venus Express VIRTIS. Icarus 211, 51–57.

Esposito, L.W., Copley, M., Eckert, R., Gates, L., Stewart, A.I.F., Worden, H., 1988. Sulfur dioxide at the Venus cloud tops, 1978–1986. J. Geophys. Res. 93, 5267–5276.

Fedorova, A. et al., 2008. HDO and H_2O vertical distributions and isotopic ratio in the Venus mesosphere by solar occultation at infrared spectrometer on board Venus Express. J. Geophys. Res. 113, E00B22.

Giauque, W.F., Hornung, E.W., Kunzler, J.E., Rubin, T.R., 1960. The thermodynamic properties of aqueous sulfuric acid solutions and hydrates from 15 to 300 K. J. Am. Chem. Soc. 82, 62–67.

Koukouli, M.E., Irwin, P.G.J., Taylor, F.W., 2005. Water vapor abundance in Venus' middle atmosphere from Pioneer Venus OIR and Venera 15 FTS measurements. Icarus 173, 84–99.

Krasnopolsky, V.A., 1980. Veneras 9 and 10: Spectroscopy of scattered radiation in the atmosphere above the clouds. Cosmic Res. 18, 899–906.

Krasnopolsky, V.A., 1983. Venus spectroscopy in the 3000–8000 Å region by Veneras 9 and 10. In: Hunten, D.M., Colin, L., Donahue, T.M., Moroz, V.I. (Eds.), Venus. Univ. Arizona Press, Tucson, pp. 459–483.

Krasnopolsky, V.A., 1986. Photochemistry of the Atmospheres of Mars and Venus. Springer, New York, 334 pp.

Krasnopolsky, V.A., 2010a. Spatially-resolved high-resolution spectroscopy of Venus. 2. Variations of HDO, OCS, and SO_2 at the cloud tops. Icarus 209, 314–322.

Krasnopolsky, V.A., 2010b. Venus night airglow: Ground-based detection of OH, observations of O_2 emissions, and photochemical model. Icarus 207, 17–27.

Krasnopolsky, V.A., Cruikshank, D.P., 1999. Photochemistry of Pluto's atmosphere and ionosphere near perihelion. J. Geophys. Res. 104, 21,979–21,996.

Krasnopolsky, V.A., Parshev, V.A., 1981. Chemical composition of the atmosphere of Venus. Nature 292, 610–613.

Krasnopolsky, V.A., Parshev, V.A., 1983. Photochemistry of the Venus atmosphere. In: Hunten, D.M., Colin, L., Donahue, T.M., Moroz, V.I. (Eds.), Venus. Univ. Arizona Press, Tucson, pp. 431–458.

Krasnopolsky, V.A., Pollack, J.B., 1994. H_2O–H_2SO_4 system in Venus' clouds and OCS, CO, and H_2SO_4 profiles in Venus' troposphere. Icarus 109, 58–78.

Lane, J.R., Kjaergaard, H.G., 2008. Calculated electronic transitions in sulfuric acid and implications for its photodissociation in the atmosphere. J. Phys. Chem. A112, 4958–4964.

Lane, W.A., Opstbaum, R., 1983. High altitude Venus haze from Pioneer Venus limb scans. Icarus 54, 48–58.

Marcq, E., Belyaev, D., Montmessin, F., Fedorova, A., Bertaux, J.L., Vandaele, A.C., Neefs, E., 2011. An investigation of the SO_2 content of the venusian mesosphere using SPICAV-UV in nadir mode. Icarus 211, 58–69.

Mills, F.P., 1998. I. Observations and Photochemical Modeling of the Venus Middle Atmosphere. II. Thermal Infrared Spectroscopy of Europa and Callsito. Ph.D. Thesis, California Institute of Technology.

Murphy, D.M., Koop, T., 2005. Review of the vapour pressures of ice and supercooled water for atmospheric applications. Quart. J. Roy. Met. Soc. 131, 1539–1565.

Parkinson, W.H., Rufus, J., Yoshino, K., 2003. Absolute absorption cross section measurements of CO_2 in the wavelength region 163–200 nm and the temperature dependence. Chem. Phys. 290, 251–256.

Richardson, C.B., Hightower, R.L., Pigg, A.L., 1986. Optical measurement of the evaporation of sulfuric acid droplets. Appl. Opt. 25, 1226–1229.

Sander, S.P. et al., 2006. Chemical Kinetics and Photochemical Data for use in Atmospheric Studies: Evaluation Number 15. JPL Publication 06-2, California Institute of Technology.

Sandor, B.J., Clancy, R.T., 2005. Water vapor variations in the Venus mesosphere from microwave spectra. Icarus 177, 129–143.

Sandor, B.J., Clancy, R.T., Moriarty-Schieven, G., Mills, F.P., 2010. Sulfur chemistry in the Venus mesosphere from SO_2 and SO microwave spectra. Icarus 208, 49–60.

Stull, D.R., 1947. Vapor pressure of pure substances—Inorganic compounds. Ind. Eng. Chem. 39, 540–550.

Tellmann, S., Pätzold, M., Häusler, B., Bird, M.K., Tyler, G.L., 2009. Structure of the Venus neutral atmosphere as observed by the Radio Science experiment VeRa on Venus Express. J. Geophys. Res. 114, E00B36.

Vaida, V., Kjaergaard, H.G., Hintze, P.E., Donaldson, D.J., 2003. Photolysis of sulfuric acid vapor by visible solar radiation. Science 299, 1566–1568.

Van de Hulst, H.C., 1957. Light Scattering by Small Particles. Wiley, New York.

Wilquet, V., Fedorova, A., Montmessin, F., Drummond, R., Mahieux, A., Vandaele, A.C., et al., 2009. Preliminary characterization of the upper haze by SPICAV/SOIR solar occultation in UV to mid-IR onboard Venus Express. J. Geophys. Res. 114, E00B42.

Woods, T.N. et al., 1996. Validation of the UARS solar ultraviolet irradiances: Comparison with the ATLAS 1 and 2 measurements. J. Geophys. Res. 101, 9541–9569.

Yung, Y.L., DeMore, W.B., 1982. Photochemistry of the stratosphere of Venus: Implications for atmospheric evolution. Icarus 51, 199–247.

Zasova, L.V., Moroz, V.I., Linkin, V.M., Khatuntsev, I.V., Maiorov, B.S., 2006. Structure of the Venusian atmosphere from surface up to 100 km. Cosmic Res. 44, 364–383.

Zeleznik, F.J., 1991. Thermodynamic properties of the aqueous sulfuric acid system to 350 K. J. Phys. Chem. Ref. Data 20, 1157–1200.

Zhang, X., Liang, M.C., Montmessin, F., Bertaux, J.L., Parkinson, C., Yung, Y.L., 2010. Photolysis of sulphuric acid as the source of sulphur oxides in the mesosphere of Venus. Nat. Geosci. 3, 834–837.